PROCEEDINGS OF THE ROYAL SOCIETY A

Proc. R. Soc. A (2006) **462**, 1387–1407
doi:10.1098/rspa.2005.1631
Published online 24 January 2006

Calculating the lift on a finite stack of cylindrical aerofoils

By Darren Crowdy*

Department of Mathematics, Imperial College London, Queen's Gate, London SW7 2AZ, UK

The classic exact solution due to Lagally (Lagally, M. 1929 Die reibungslose strömung im aussengebiet zweier kreise. *Z. Angew. Math. Mech.* **9**, 299–305.) for streaming flow past two cylindrical aerofoils (or obstacles) is generalized to the case of an arbitrary finite number of cylindrical aerofoils. Given the geometry of the aerofoils, the speed and direction of the oncoming uniform flow and the individual round-aerofoil circulations, the complex potential associated with the flow is found in analytical form in a parametric pre-image region that can be conformally mapped to the fluid region. A complete determination of the flow then follows from knowledge of the conformal mapping between the two regions. In the special case where the aerofoils are all circular, the conformal mapping from the parametric pre-image region to the fluid domain is a Möbius mapping. The solution for the complex potential in such a case can then be used, in combination with the Blasius theorem, to compute the distribution of hydrodynamic forces on the multi-aerofoil configuration.

Keywords: multiple aerofoils; lift; Kutta–Joukowski; Schottky; Klein

1. Introduction

The problem of steady streaming flows past objects—or aerofoils—is an important basic problem in elementary fluid dynamics and of fundamental importance in aerodynamics. Perhaps still one of the clearest presentations of the early theory of aerofoils from the first quarter of the twentieth century is the classic monograph by Glauert (1947). This reference includes background on the basic theory of two-dimensional aerofoils featuring chapters on monoplane aerofoils (consisting of a single aerofoil in a planar flow), biplane aerofoils (comprising two aerofoils) and even a chapter on interference effects on aerofoils due to the walls of a wind tunnel. Another good reference to the fundamentals of wing theory, including discussions of the biplane case (which is particularly relevant to what follows), is the monograph by Robinson (1956).

One of the basic results of aerofoil theory is the Kutta–Joukowski lift theorem (Milne-Thomson 1968; Acheson 1990) stating that the vertical lift force, F_y say, on a single aerofoil of arbitrary shape in a uniform flow with speed U is

$$F_y = -\rho\Gamma U, \tag{1.1}$$

*d.crowdy@imperial.ac.uk

Received 15 August 2005
Accepted 29 November 2005

where ρ is the density of the fluid and Γ is the circulation around the aerofoil. This result is most easily derived by considering the complex potential $w(z)$, where $z=x+\mathrm{i}y$, for the steady potential flow exterior to the aerofoil and combining this with the Blasius theorem (Acheson 1990) which provides a formula for the complex force on the aerofoil in the form

$$F_x - \mathrm{i}F_y = \frac{\mathrm{i}\rho}{2}\oint_{\partial D}\left(\frac{\mathrm{d}w}{\mathrm{d}z}\right)^2 \mathrm{d}z, \tag{1.2}$$

where F_x is the horizontal force component and ∂D denotes the aerofoil boundary. As usual, $w(z)=\phi(x, y)+\mathrm{i}\psi(x, y)$, where φ and ψ are, respectively, the velocity potential and streamfunction associated with the incompressible flow. The velocity field is $\boldsymbol{u}=(u, v)$, where $u-\mathrm{i}v=\mathrm{d}w/\mathrm{d}z$.

In the case of a single circular aerofoil of unit radius, the complex potential is well-known to be given by

$$w(z) = U\left(z+\frac{1}{z}\right) - \frac{\mathrm{i}\Gamma}{2\pi}\log z. \tag{1.3}$$

On substitution of (1.3) into (1.2), the result is

$$F_x - \mathrm{i}F_y = \mathrm{i}\rho\Gamma U, \tag{1.4}$$

which yields the lift force (1.1), as well as the result that the aerofoil experiences zero drag. The latter result is known as D'Alembert's paradox/theorem.

The proof of the Kutta–Joukowski theorem relies on the fact that the integration contour around the aerofoil can be deformed (by Cauchy's theorem) away from the aerofoil and around the point at infinity where it is seen that the residue there is always independent of the shape of the aerofoil (the calculation reduces, in essence, to the computation of a residue of the integrand at infinity). This proof fails, however, when multiple aerofoils are present: when computing the lift around any one of the aerofoils the other aerofoils impede the process of being able to continuously deform the contour surrounding the chosen aerofoil to a contour around the point at infinity. The lift force on a particular aerofoil is therefore no longer derivable from a simple residue calculation at infinity. Rather, it now depends in a rather complicated way on the global geometry of the aerofoil configuration, the far-field flow conditions and the separate round-aerofoil circulations. In light of this, it is of some advantage to have at hand a flexible analytical approach to the computation of such lift forces. This paper presents such an approach.

The Kutta–Joukowski lift force result (1.1) also holds in the case of an infinite, vertically periodic stack of identical aerofoils (Acheson 1990). This can be demonstrated by considering a momentum balance argument, based on an integrated form of the Euler equation, in a periodic control volume containing just a single aerofoil. A further consequence of the same argument is that each aerofoil experiences a non-zero drag force (Acheson 1990).

But what happens between these two extremes of a single aerofoil and an infinite periodic array of aerofoils? What are the forces on a finite number of aerofoils placed in an oncoming streaming flow and around which there may exist non-zero circulatory flows? While it remains true that the total lift, summed over

all aerofoils, on a finite stack will be furnished by the Kutta–Joukowski result $-\rho\Gamma_T U$, where Γ_T denotes the sum of circulations around all the aerofoils, and also that the total drag on the multi-component system will be zero, there will nevertheless be an (in general, complicated) internal distribution of hydrodynamic forces acting on the individual components of the aerofoil system. In the wing theory literature, such internal force distributions are referred to as *interference* forces (Robinson 1956). The determination of such forces is important in the structural design of multi-component aerofoils since it is usually required that the aerofoil configuration remains rigid so that the internal forces on a configuration of aerofoils must be appropriately counterbalanced (in a third dimension, so to speak) if the configuration is to remain rigid.

In the case of a finite stack of aerofoils, the lack of any periodicity obstructs a straightforward generalization of the above-mentioned momentum balance argument to determine the forces on individual aerofoils since the streamline distribution now has a complicated (aperiodic and asymmetric) structure. It therefore becomes generally impossible to invoke any symmetry arguments to identify an appropriate control volume in the flow that can yield any definite quantitative information on the force balance. Indeed, the only way to determine forces in this case is by direct calculation performed, most conveniently, by exploiting the Blasius theorem. But this requires a determination of the relevant complex potential, $w(z)$, governing the flow around the aerofoils.

For a single aerofoil, up to conformal mapping, the solution is given by (1.3). Lagally (1929) presented an analytical solution to the problem of uniform flow past two circular obstacles, a solution in which both round-obstacle circulations can be individually specified. At about the same time, Ferrari (1930) considered the same two-obstacle problem by finding a conformal mapping from the exterior of two circular discs to the exterior of two parallel line segments. Lagally's solution makes use of the theory of elliptic functions and is an elegant extension of the single obstacle solution (1.3). Of course, Lagally's solution lends itself naturally to the calculation of lift on biplane aerofoils and this was recognized, and implemented, by Garrick (1936) who constructed the relevant conformal mappings needed to complete the solution. Analytical solutions for more than two aerofoils do not appear to have been reported previously in the literature.

This paper presents analytical formulae for the complex potentials when there are more than two aerofoils, thereby generalizing Lagally's solution to any finite number of aerofoils. The method is to introduce a parametric ζ-plane and to determine the required complex potential, $W(\zeta)=w(z(\zeta))$, as a function of ζ in some bounded multiply connected circular domain which we call D_ζ. D_ζ maps, under some conformal mapping $z(\zeta)$, to the unbounded domain, here called D_z, outside any given finite arrangement of aerofoils. It is known, from general results in conformal mapping theory, that any such D_z is conformally equivalent (in the manner just described) to *some* choice of multiply connected circular domain D_ζ. Moreover, the boundary value problem we solve here for the complex potential in D_ζ is conformally invariant. This means that the complex potential $W(\zeta)$ is then also the required complex potential around the aerofoils in the domain D_z. As a result, up to knowledge of the conformal mapping $z(\zeta)$, the solution to the problem in the fluid domain D_z is complete.

We restrict attention here to a study of examples involving circular aerofoils since, in such a case, the mapping $z(\zeta)$ from the circular domain D_ζ to D_z is then

just a linear fractional transformation (or Möbius mapping) which is easily determined. With analytical knowledge of both $W(\zeta)$ and $z(\zeta)$, the Blasius theorem can be directly employed to calculate the forces on each of the aerofoils.

Finally, we remark that while we have elected to present these results in the context of aerodynamics, the mathematical results have relevance in many other areas. For example, there are civil engineering applications where it is important to compute the forces due to steady laminary flow around a series of obstacles (such as bridge piers or offshore drill rig supports). Yamamoto (1976) lists a number of other real flow situations in which this idealized flow model is relevant. Some further applications to geophysical fluid dynamics are discussed later in §10.

2. A finite stack of aerofoils

Consider the unbounded region D_z exterior to a collection of $M+1$ aerofoils of bounded extent. The aerofoils will be denoted $\{D_j|j=0, 1, \ldots, M\}$ and their boundaries will be $\{\partial D_j|j=0, 1, \ldots, M\}$. The region D_z will be supposed to be filled with an incompressible fluid, of density ρ, in steady irrotational motion. It is supposed that the aerofoils are sitting in a uniform flow with speed U and making angle χ to the positive real axis. Suppose that there is a circulation Γ_k around the kth aerofoil D_k. Such a combination of a streaming flow with a non-zero round-aerofoil circulation is expected to produce lift forces on the aerofoils.

To make progress in solving this problem, let D_ζ be a bounded circular domain in a parametric ζ-plane. A circular domain is a domain whose boundaries are all circular. Let the outer boundary, given by $|\zeta|=1$, be called C_0. Let M be a non-negative integer and let the boundaries of M smaller circular discs enclosed by C_0 be denoted $\{C_j|j=1, \ldots, M\}$. $M=0$ will correspond to the single aerofoil case in which there are no enclosed circular discs and the pre-image domain D_ζ is just the unit ζ-disc. Let the radius of circle C_j be $q_j\in\mathbb{R}$ and let its centre be at $\delta_j\in\mathbb{C}$. Such a domain D_ζ is $(M+1)$-connected.

It will be supposed that $z(\zeta)$ is a conformal mapping from *some* circular domain D_ζ to the fluid region D_z. The values of the parameters $\{q_j, \delta_j|j=1, \ldots, M\}$ will be determined by the choice of the target domain D_z. Since D_z is unbounded there must be some point in D_ζ at which $z(\zeta)$ has a simple pole. This point will be the pre-image of the point $z=\infty$. Suppose $\zeta=\beta$ is this point and that, as $\zeta\to\beta$,

$$z(\zeta) = \frac{a}{\zeta-\beta} + \mathcal{O}(1) \tag{2.1}$$

for some constant a. A rotational degree of freedom of the Riemann mapping theorem allows us to assume a is real. The point β can be chosen arbitrarily.

Solving the above flow problem in the region D_z exterior to the aerofoils $\{D_j|j=0, 1, \ldots, M\}$ is equivalent to finding a function $w(z)$, a complex potential that is analytic everywhere in D_z except at infinity where

$$w(z) \sim U\,\mathrm{e}^{-\mathrm{i}\chi} z + \mathcal{O}(1), \quad \text{as } z\to\infty \tag{2.2}$$

for real constants U and χ. Condition (2.2) ensures that the flow speed at infinity is U and makes an angle χ with the positive real axis. $w(z)$ must also satisfy the

boundary conditions that $\mathrm{Im}[w(z)]$ is constant on the aerofoil boundaries. The latter conditions ensure that all the aerofoil boundaries are streamlines. These constant values can, in general, be different on the different aerofoils and these degrees of freedom are associated with the freedom to specify the round-aerofoil circulations. Here, the constants will be determined by the conditions, stipulated earlier, that the circulation around D_j is Γ_j.

The aim is to find $w(z)$ as a function of ζ in the region D_ζ; that is, the function $W(\zeta, \beta) \equiv w(z(\zeta))$ will be determined. The notation reflects the dependence of the complex potential on the choice of the point β in D_ζ mapping to infinity. By linear superposition, $W(\zeta, \beta)$ is the sum of a complex potential $W_U(\zeta, \beta)$ corresponding to the uniform streaming flow and a complex potential $W_\Gamma(\zeta, \beta)$ associated with the imposed circulations around the aerofoils, i.e.

$$W(\zeta, \beta) = W_U(\zeta, \beta) + W_\Gamma(\zeta, \beta). \tag{2.3}$$

$W(\zeta, \beta)$ must be analytic (but not necessarily single-valued) everywhere in D_ζ. It must also be such that

$$\mathrm{Im}[W(\zeta, \beta)] = \gamma_j, \quad \text{on } C_j, \quad j = 0, 1, \ldots, M, \tag{2.4}$$

where $\{\gamma_j | j = 0, 1, \ldots, M\}$ are a set of constants.

3. The special function $\omega(\zeta, \gamma)$

To construct $W_U(\zeta, \beta)$ and $W_\Gamma(\zeta, \beta)$ a special transcendental function $\omega(\zeta, \gamma)$ associated with the choice of circular domain D_ζ will be needed. It was introduced in Crowdy & Marshall (2005*a*), and further exploited in Crowdy & Marshall (2005*b*), to study problems arising in the motion of point vortices in bounded multiply connected domains. Here, we briefly review its definition.

Given some circular domain D_ζ uniquely specified by some choice of the parameters $\{(q_j, \delta_j) | j = 1, \ldots, M\}$, define the set of M Möbius maps given by

$$\theta_j(\zeta) = \frac{a_j \zeta + b_j}{c_j \zeta + d_j}, \quad j = 1, \ldots, M, \tag{3.1}$$

where

$$a_j = q_j - \frac{|\delta_j|^2}{q_j}, \quad b_j = \frac{\delta_j}{q_j}, \quad c_j = -\frac{\bar{\delta}_j}{q_j}, \quad d_j = \frac{1}{q_j}. \tag{3.2}$$

These M maps, together with their inverses which are also Möbius maps, can be composed in an infinite number of ways to generate an infinite group of Möbius maps. See Crowdy & Marshall (2005*a*) for more details. This infinite group of Möbius maps can be used to define the special function $\omega(\zeta, \gamma)$ as an infinite product. Indeed, $\omega(\zeta, \gamma)$ is defined to be

$$\omega(\zeta, \gamma) = (\zeta - \gamma)\omega'(\zeta, \gamma), \tag{3.3}$$

where

$$\omega'(\zeta, \gamma) = \prod_{\theta_k} \frac{(\theta_k(\zeta) - \gamma)(\theta_k(\gamma) - \zeta)}{(\theta_k(\zeta) - \zeta)(\theta_k(\gamma) - \gamma)}, \tag{3.4}$$

and where the product is over all compositions of the basic maps $\{\theta_j, \theta_j^{-1} | j = 1, \ldots, M\}$ excluding the identity map and all inverse maps. For more information on this function the reader should consult Crowdy & Marshall (2005*a*,*b*). The function is also discussed, in a much more general context, in ch. 12 of Baker (1995).

4. Complex potential for uniform flow

It is shown in Crowdy (in press) that the complex potential for uniform flow, with speed U and making an angle χ with the positive real axis, is

$$W_U(\zeta, \beta) = Ua\left[e^{i\chi}\frac{\partial}{\partial\bar{\beta}} - e^{-i\chi}\frac{\partial}{\partial\beta}\right] W_0(\zeta, \beta), \tag{4.1}$$

where

$$W_0(\zeta, \beta) = \log\left(\frac{\omega(\zeta, \beta)}{|\beta|\omega(\zeta, \bar{\beta}^{-1})}\right), \tag{4.2}$$

This result will be used here without proof. The reader is referred to Crowdy (in press) for the derivation.

5. Imposing round-aerofoil circulations

The following section describes the principal new mathematical results of this paper. Suppose it is required to impose circulation Γ_k around the obstacle D_k. The complex potential corresponding to this will be denoted $W_\Gamma(\zeta)$. It is given by the formula

$$W_\Gamma(\zeta, \beta) = \sum_{k=0}^{M} \frac{i\Gamma_k}{2\pi} \log R_k(\zeta, \beta), \tag{5.1}$$

where

$$R_k(\zeta, \beta) = \frac{\omega(\zeta, \beta)}{\omega(\zeta, \theta_k(\bar{\beta}^{-1}))}, \quad k = 0, 1, \ldots, M, \tag{5.2}$$

and where, in addition to the maps $\{\theta_k | k = 1, \ldots, M\}$ defined in §3, we define $\theta_0(\zeta)$ to be the identity map, i.e. $\theta_0(\zeta) = \zeta$.

It is important to note that $R_k(\zeta, \beta)$ has a simple zero at the point $\zeta = \beta$ and a simple pole at the point $\theta_k(\bar{\beta}^{-1})$. On use of properties of the maps $\{\theta_k | k = 1, \ldots, M\}$ described in detail in Crowdy & Marshall (2005*a*), it turns out that the latter point corresponds to the reflection of the point β in the circle C_k. As a result, the simple pole of $R_k(\zeta, \beta)$ does *not* lie in the circular region D_ζ; rather, it lies inside the circle C_k. To understand this, note that if one maps the region D_ζ using the reflection mapping $\zeta \mapsto \bar{\zeta}^{-1}$ then the image lies in a region exterior to the unit disc in the ζ-plane. Under a further composition with the mapping θ_k this region exterior to the unit disc is mapped to a bounded region inside the circle C_k (this is how we deduce that the point $\theta_k(\bar{\beta}^{-1})$ is inside C_k). It turns out that the union of the latter region and the original region D_ζ constitute what is known as a *fundamental region* for the group of transformations generated by the maps and their inverses. This means that the whole of the complex plane can be tessellated by the images, under

all the maps generated by the basic maps $\{\theta_j | j=1, \ldots, M\}$, of this fundamental region. It is natural to choose the branch of the logarithm in each term of the sum in (5.1) so that the zero at $\zeta=\beta$ is joined by a branch cut to the pole at $\zeta=\theta_k(\bar{\beta}^{-1})$ in the fundamental region and that the image of this pair of points in each of the 'image regions' of the fundamental region should similarly be joined pairwise by branch cuts.

Having chosen the branch in this way, to get a circulation Γ_k around the aerofoil corresponding to C_k we must construct a function with a logarithmic singularity of strength $-\mathrm{i}\Gamma_k/2\pi$ inside the aerofoil D_k. This is so that the change in argument of this function as the aerofoil D_k is traversed in an anticlockwise sense is Γ_k. Since going anticlockwise around any of the interior circles $\{C_k | k=1, \ldots, M\}$ corresponds to going anticlockwise around the cylinders D_k, it is natural to consider the function given by

$$\sum_{k=1}^{M} -\frac{\mathrm{i}\Gamma_k}{2\pi} \log[R_k(\zeta, \beta)]^{-1}. \tag{5.3}$$

Also, since going anticlockwise around D_0 means that C_0 must be traversed in a clockwise direction, it is natural to add in the contribution

$$-\left(\frac{-\mathrm{i}\Gamma_0}{2\pi}\right) \log R_0(\zeta, \beta). \tag{5.4}$$

The total complex potential $W_\Gamma(\zeta, \beta)$ given in (5.1) is then the sum of (5.3) and (5.4).

While (5.1) has the correct distribution of logarithmic singularities, it remains to ascertain that it satisfies the additional requirement that it has constant imaginary part on the circles $\{\mathrm{C}_k | k=0, 1, \ldots, M\}$. These important conditions can be seen to be satisfied by (5.1) on use of some transformation properties of the special function $\omega(\zeta, \cdot)$ reported in Crowdy & Marshall (2005*a*). The details are omitted here since the proofs are very similar to proofs of related results presented in detail in Crowdy & Marshall (2005*a*); we refer the reader there for an indication of how to demonstrate this result analytically. To substantiate the result here however, we offer some numerical corroboration. Figure 1 shows graphs of the imaginary parts of $W(\zeta, \beta)$, evaluated on the boundaries of three cylinders (each of unit radius and centred at $0, \pm 4$) for the example situation in which $U=1$, $\Gamma_0=\Gamma_1=\Gamma_2=-5$ and $\chi=0$ (we have also arbitrarily taken $\beta=0.1$). The graphs in figure 1 have been computed by truncating the infinite product defining the function $\omega(\zeta, \beta)$ at level four (keeping all Möbius maps up to level 3 and ignoring all higher-level mappings. For an explanation of this terminology, see Crowdy & Marshall (2005*a*)).

6. Calculation of the forces on the aerofoils

By the Blasius theorem (Milne-Thomson 1968), if $w(z)$ is the complex potential for flow past an obstacle with boundary ∂D, then the complex force $F_x - \mathrm{i}F_y$ exerted by the fluid of density ρ on the body is given in (1.2). Let $F_x^{(j)} - \mathrm{i}F_y^{(j)}$ denote the complex force exerted by the fluid on the jth aerofoil. Then it follows that

$$F_x^{(j)} - \mathrm{i}F_y^{(j)} = \frac{\mathrm{i}\rho}{2} \oint_{\partial D_j} \left(\frac{\mathrm{d}w}{\mathrm{d}z}\right)^2 \mathrm{d}z. \tag{6.1}$$

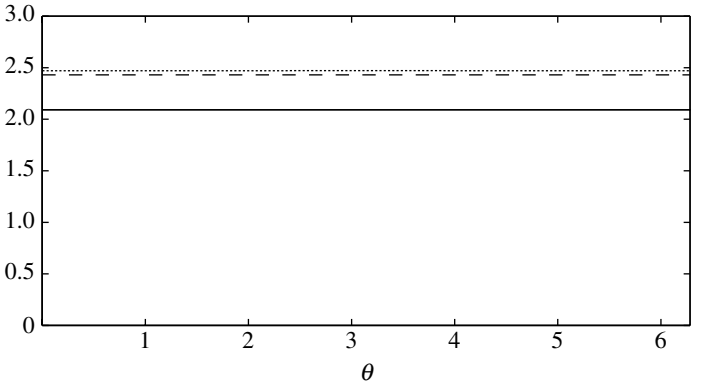

Figure 1. Graph showing the imaginary parts of the complex potential $W(\zeta,\beta)=W_U(\zeta,\beta)+W_r(\zeta,\beta)$ as a function of θ, where points on the jth circle C_j are parameterized by $\delta_j+q_j\,\mathrm{e}^{\mathrm{i}\theta}$. The cylinders all have unit radius and are centred at 0, ±4. The solid line corresponds to the values on the central cylinder, the dotted and dashed lines corresponds to values on the cylinders with centres 4 and -4, respectively. Here $U=1$, $\Gamma_0=\Gamma_1=\Gamma_2=-5$, $\chi=0$ (and we have taken $\beta=0.1$).

It follows, in turn, that

$$F_x^{(0)}-\mathrm{i}F_y^{(0)}=-\frac{\mathrm{i}\rho}{2}\oint_{C_0}\left(\frac{\mathrm{d}W}{\mathrm{d}\zeta}\right)^2\left(\frac{\mathrm{d}z}{\mathrm{d}\zeta}\right)^{-1}\mathrm{d}\zeta, \tag{6.2}$$

while for $j=1,\ldots,M$,

$$F_x^{(j)}-\mathrm{i}F_y^{(j)}=\frac{\mathrm{i}\rho}{2}\oint_{C_j}\left(\frac{\mathrm{d}W}{\mathrm{d}\zeta}\right)^2\left(\frac{\mathrm{d}z}{\mathrm{d}\zeta}\right)^{-1}\mathrm{d}\zeta, \tag{6.3}$$

where, on changing variables in the integrals, account has been taken of any change in sense of the direction of integration. The most effective way to compute the lift based on (6.2) and (6.3) is to use the analytical expressions for $W(\zeta,\beta)$ determined earlier and to perform the numerical quadrature using the trapezoidal rule which gives exponential accuracy for periodic functions integrated over a period, which is the precisely the case here once the contour integrals are parameterized in terms of θ, where $\zeta=\delta_j+q_j\,\mathrm{e}^{\mathrm{i}\theta}$. The calculation of torques, especially on non-circular obstacles, can be computed in a similar way if required.

7. The case of a single aerofoil

To retrieve the well-known result (1.3) within the context of the present theory note that, in the simply connected case, there are no enclosed circular discs and therefore no non-trivial Möbius maps. Thus, $\omega(\zeta,\gamma)=(\zeta-\gamma)$. Making the choice $\beta=0$ then leads, after some manipulation, to (1.3). Typical streamlines, for different values of the round-aerofoil circulation, are shown in figure 2. An important feature is that, as the circulation increases, two stagnation points on the aerofoil move to the lower side of the aerofoil until, at a critical value of the circulation, they coalesce and move off the aerofoil into the flow.

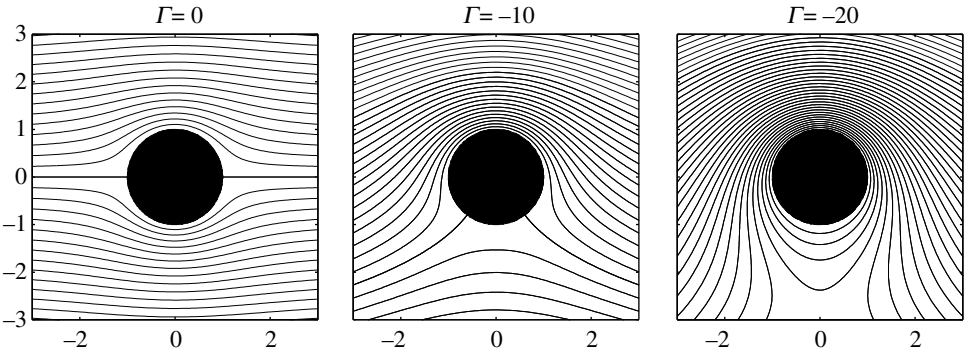

Figure 2. Uniform flow past a single unit-radius cylindrical aerofoil with $U=1$ and $\Gamma=0$, -10 and -20. As the circulation becomes increasingly negative the two stagnation points move to the lower side of the cylinder and, when the circulation is sufficiently strong, coalesce and move off the aerofoil into the flow.

8. The case of two (biplane) aerofoils

It is instructive to examine how the general theory just presented retrieves known formulae in the biplane case comprising two aerofoils. In this way, we reproduce the classic solution of Lagally (1929) who, in contrast to our own function theoretic approach, employed the theory of elliptic functions. It should also be mentioned that, with geophysical (rather than aerodynamical) motivation in mind, Johnson & McDonald (2004) have generalized the Lagally solution to include the effects of a finite set of point vortices evolving in the flow around two circular islands.

It is well-known that any doubly connected domain is conformally equivalent to an annular region $q<|\zeta|<1$ for some value of the conformal modulus q (Nehari 1952). In this case, $\delta_1=0$ and $q_1=q$, so that the relevant Möbius map is $\theta_1(\zeta)=q^2\zeta$. It can then be shown that

$$\omega(\zeta,\gamma)=-\frac{\gamma}{C^2}P(\zeta/\gamma,q), \tag{8.1}$$

where

$$P(\zeta,q)\equiv(1-\zeta)\prod_{k=1}^{\infty}(1-q^{2k}\zeta)(1-q^{2k}\zeta^{-1}),\quad C\equiv\prod_{k=1}^{\infty}(1-q^{2k}). \tag{8.2}$$

It is straightforward to verify, directly from the definition (8.2), that

$$P(\zeta^{-1},q)=-\zeta^{-1}P(\zeta,q),\quad P(q^2\zeta,q)=-\zeta^{-1}P(\zeta,q). \tag{8.3}$$

It follows that

$$\left.\begin{aligned}R_0(\zeta,\beta)&=\frac{\omega(\zeta,\beta)}{\omega(\zeta,\bar{\beta}^{-1})}=|\beta|^2\frac{P(\zeta\beta^{-1},q)}{P(\zeta\bar{\beta},q)},\\ R_1(\zeta,\beta)&=\frac{\omega(\zeta,\beta)}{\omega(\zeta,q^2\bar{\beta}^{-1})}=\frac{|\beta|^2}{q^2}\frac{P(\zeta\beta^{-1},q)}{P(\zeta\bar{\beta}q^{-2},q)}.\end{aligned}\right\} \tag{8.4}$$

Suppose now that it is required to impose a circulation Γ_0 around the obstacle corresponding to C_0 and a circulation Γ_1 around the obstacle corresponding to C_1. Then, by the theory presented above, the associated complex potential is

$$W_T(\zeta,\beta) = \frac{\mathrm{i}\Gamma_0}{2\pi}\log R_0(\zeta,\beta) + \frac{\mathrm{i}\Gamma_1}{2\pi}\log R_1(\zeta,\beta). \tag{8.5}$$

On use of the properties (8.3) it can then be shown that $R_1(\zeta,\alpha) \propto \zeta^{-1}R_0(\zeta,\alpha)$. This implies that, to within an unimportant constant, (8.5) is equivalent to

$$W_T(\zeta,\beta) = \frac{\mathrm{i}(\Gamma_0+\Gamma_1)}{2\pi}\log R_0(\zeta,\beta) - \frac{\mathrm{i}\Gamma_1}{2\pi}\log\zeta. \tag{8.6}$$

The conformal mapping from the annulus $q<|\zeta|<1$ to two equal obstacles, of unit radius, symmetrically disposed with respect to the origin on the real axis is given by

$$z(\zeta) = R\left(\frac{1-q}{4\sqrt{q}}\right)\left[\frac{\zeta+\sqrt{q}}{\zeta-\sqrt{q}}\right], \tag{8.7}$$

where $R=1$ if considering two aerofoils aligned along the x-axis or $R=-\mathrm{i}$ if considering vertically aligned aerofoils. It is clear that, in respect of (2.1), we can identify

$$\beta = \sqrt{q}, \quad a = \frac{R(1-q)}{2}. \tag{8.8}$$

Adjusting q changes the separation of the two unit-radius aerofoils. The contribution, $W_U(\zeta,\beta)$, to the complex potential due to the uniform flow is

$$W_U(\zeta,\sqrt{q}) = U\left(\frac{1-q}{2\sqrt{q}}\right)\left[\mathrm{e}^{-\mathrm{i}\chi}K(\zeta/\sqrt{q},q) - \mathrm{e}^{\mathrm{i}\chi}K(\zeta\sqrt{q},q)\right], \tag{8.9}$$

where

$$K(\zeta,q) \equiv \frac{\zeta P_\zeta(\zeta,q)}{P(\zeta,q)}. \tag{8.10}$$

The total complex potential can therefore be written

$$\begin{aligned} W(\zeta,\beta) = {} & \frac{\mathrm{i}(\Gamma_0+\Gamma_1)}{2\pi}\log R_0(\zeta,\sqrt{q}) - \frac{\mathrm{i}\Gamma_1}{2\pi}\log\zeta \\ & + U\left(\frac{1-q}{2\sqrt{q}}\right)\left[\mathrm{e}^{-\mathrm{i}\chi}K(\zeta/\sqrt{q},q) - \mathrm{e}^{\mathrm{i}\chi}K(\zeta\sqrt{q},q)\right]. \end{aligned} \tag{8.11}$$

The complex potential, $W_L(Z)$ say, given by Lagally (1929) as a function of a complex variable Z, takes the form

$$W_{\mathrm{L}}(Z) = -\frac{\mathrm{i}\Gamma}{2\pi}\log\left(\frac{\sigma(Z)}{\sigma(Z+2\gamma)}\right) + 2c(w_\infty\zeta(Z) - \overline{w_\infty}\zeta(Z+2\gamma)) + \mathrm{i}\kappa Z, \tag{8.12}$$

where Γ, γ, c, w_∞ and κ are appropriate constants, while $\sigma(Z)$ and $\zeta(Z)$ represent the Weierstrass sigma and zeta functions, respectively (Whittaker & Watson 1927). Identifying the complex variable Z with $\log\zeta$, the function $P(\zeta,q)$ with the Weierstrass σ-function, the function $K(\zeta,q)$ with the Weierstrass ζ-function and with appropriate identification of constants, it can be shown that (8.11) is equivalent to Lagally's solution (8.12).

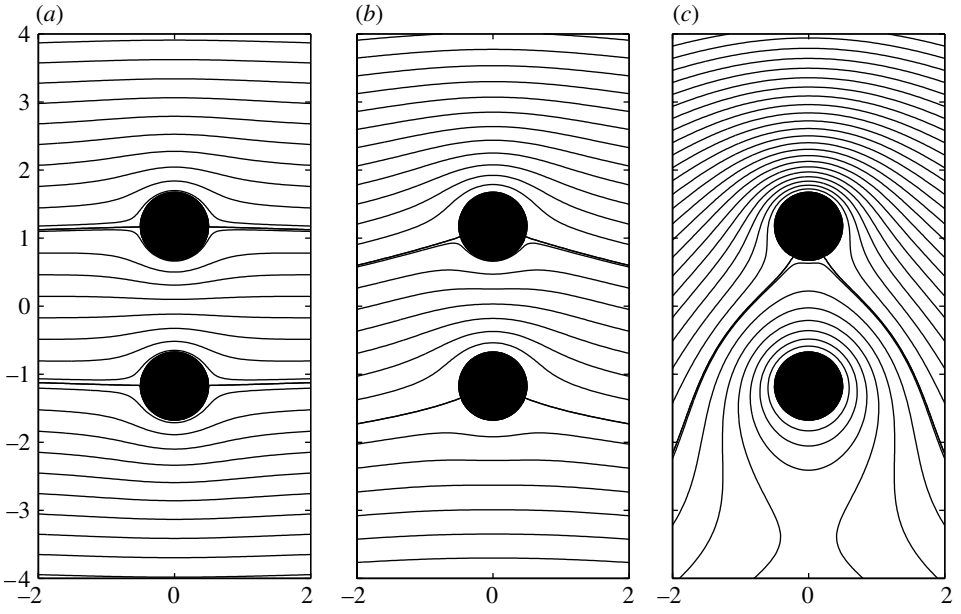

Figure 3. Streamline distribution past two equal cylindrical vertically aligned aerofoils, with unit diameter, corresponding to $\rho=0.05$ with $U=1$, $\chi=0$ and (*a*) $\Gamma_0=\Gamma_1=0$, (*b*) -1 and (*c*) -5. The centres of the aerofoils are at $\pm 1.1739\mathrm{i}$. The lower aerofoil corresponds to the image of C_0. Streamlines drawn at intervals of 0.3.

(*a*) *Unstaggered biplane aerofoils*

Figure 3 depicts several streamline distributions associated with uniform flow of strength $U=1$ parallel to the x-axis (so that $\chi=0$) past two identical vertically aligned circular aerofoils of unit radius. Glauert (1947) describes such a configuration of aerofoils as 'unstaggered biplane aerofoils'. The value of $\rho=0.05$ is chosen arbitrarily (so the distance of the centre of each aerofoil from the origin turns out to be 1.1763). The circulations around each aerofoil are assumed to be equal so that $\Gamma_0=\Gamma_1=\Gamma$ and the figure shows the three cases $\Gamma=0$, -1 and -5. As for the forces, neither aerofoil experiences any drag. This is to be expected since, by Bernoulli's theorem, the pressure distribution p is given by

$$p = H-\frac{1}{2}|\boldsymbol{u}|^2 = H-\frac{1}{2}\left|\frac{\mathrm{d}w}{\mathrm{d}z}\right|^2 = H-\frac{1}{2}\left|\left(\frac{\mathrm{d}W}{\mathrm{d}\zeta}\right)\left(\frac{\mathrm{d}z}{\mathrm{d}\zeta}\right)^{-1}\right|^2, \tag{8.13}$$

where H is the Bernoulli constant. However, it is clear from the streamline distribution in figure 3 that the velocity field is symmetric fore and aft of the centreline of the vertical stack of aerofoils so any net force on any of them can only act vertically.

Figure 4 graphs these vertical forces on the two aerofoils as functions of the separations of the aerofoil centres. The case $\Gamma=0$ is shown and reveals that, even with no circulation around either of the aerofoils, there is a net lift on the lower aerofoil and a net downward force on the upper aerofoil. Thus, the presence of a neighbouring aerofoil clearly causes an increase in streaming velocity of the fluid in the gap between the aerofoils thereby decreasing the fluid pressure there

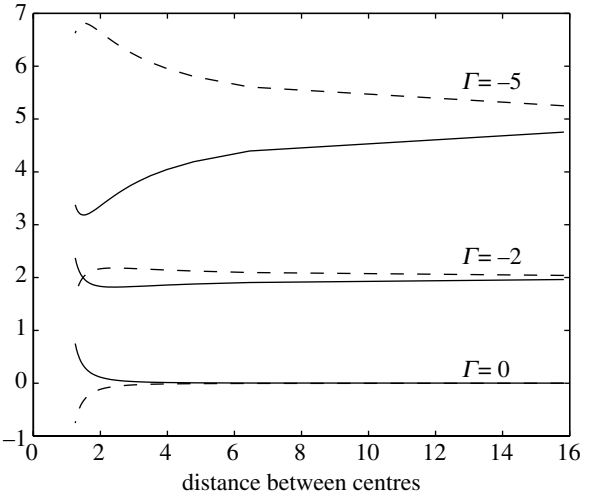

Figure 4. Graph of lift force on aerofoils in the vertically aligned configuration with $U=1$, $\chi=0$ and three different values of $\Gamma_0=\Gamma_1=\Gamma$. The solid line denotes the lift force on the lower aerofoil, the dashed line the lift on the upper aerofoil. Note that, even with no circulation, there are vertical forces on the two aerofoils. At all separations the sum of the vertical lift forces equals twice the Kutta–Joukowski value.

(by Bernoulli's theorem). This leads to a net attractive force between the aerofoils. This is a manifestation of a phenomenon sometimes referred to as 'ground effect': in this symmetrical case of streaming flow past the two equal cylinders, the lower aerofoil can be interpreted as an 'image' aerofoil and the central straight streamline which perpendicularly bisects the line-of-centres between the aerofoils can effectively be replaced by a wall or runway (i.e. the 'ground'). The effect of the ground ('ground effect') is to pull the aerofoil towards it. The same phenomenon is observed by Yamamoto (1976) and Wang (2004).

As the circulation Γ around the aerofoils increases it is seen that, eventually, the lift forces on the upper aerofoil dominate those on the lower aerofoil at all values of the separation. Two things should be noted: first, as the separation of the aerofoils tends to infinity the lift on each aerofoil tends to the Kutta–Joukowski value of $-\rho\Gamma U$; second, irrespective of their separation, the sum of their respective lift forces always equals twice the Kutta–Joukowski value. This is to be expected from a straightforward application of the Blasius theorem to both aerofoils and a deformation of the associated integration contour, justified by Cauchy's theorem, to a large contour surrounding the point at infinity (just as in the proof of the Kutta–Joukowski theorem in the case of a single aerofoil).

(*b*) *Tandem biplane aerofoils*

Figure 5 shows streamline distributions in the case where the two equal aerofoils are now aligned in the direction of the flow (i.e. horizontally). Glauert (1947) refers to this geometrical arrangement as 'tandem aerofoils'. The round-aerofoil circulations are taken to be equal. As this circulation value increases, it is again observed that the two stagnation points on each aerofoil move to the lower side of each aerofoil until they eventually move off into the flow.

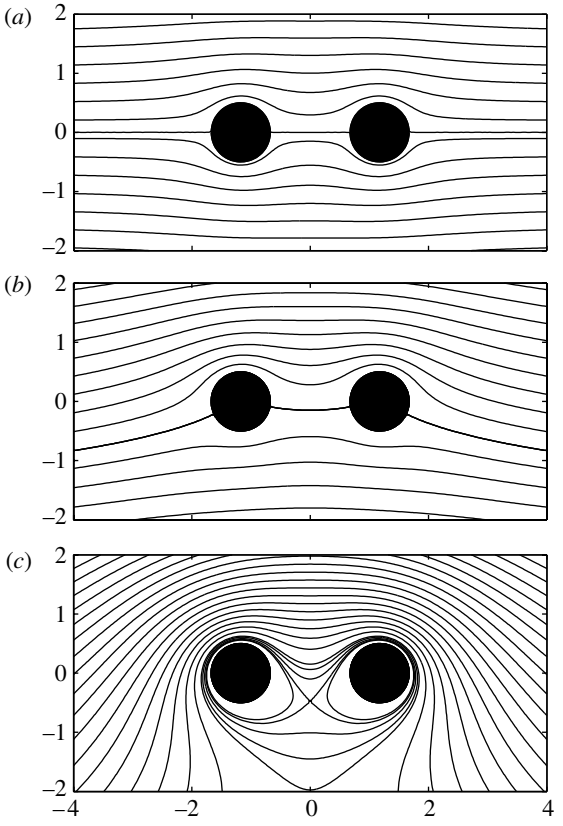

Figure 5. Streamline distribution past two equal cylindrical horizontally aligned aerofoils, with unit diameter, corresponding to $\rho=0.05$ with $U=1$, $\chi=0$ and (*a*) $\Gamma_0=\Gamma_1=0$, (*b*) -1 and (*c*) -5. The centres of the aerofoils are at ± 1.1739. The right-most aerofoil corresponds to the image of C_0. Streamlines drawn at intervals of 0.3.

As for the forces in this case, since it is known that the total lift force must sum to twice the Kutta–Joukowski value whatever the separation of the aerofoils, it follows from the symmetry of the configuration that the lift on each aerofoil must equal the Kutta–Joukowski value regardless of how far apart the aerofoils are. This is found to be the case. It is the horizontal forces that are more interesting in this case. Of course, since the total horizontal force on the two-aerofoil configuration must be zero, if there are any horizontal forces on each aerofoil they must be equal and opposite. This is found to be the case. Figure 6 graphs the horizontal force on the right-hand aerofoil as a function of separation of the aerofoils. In contrast to the vertical alignment, when horizontally aligned the aerofoils are found to repel each other, the strength of repulsion increasing as the separation decreases. This means that in the gap between the aerofoils the overall fluid speed must be smaller than that to either side thereby leading to higher pressures in the gap region (by Bernoulli's theorem). Again, Yamamoto (1976) and Wang (2004) have observed the same phenomenon using rather separate methods.

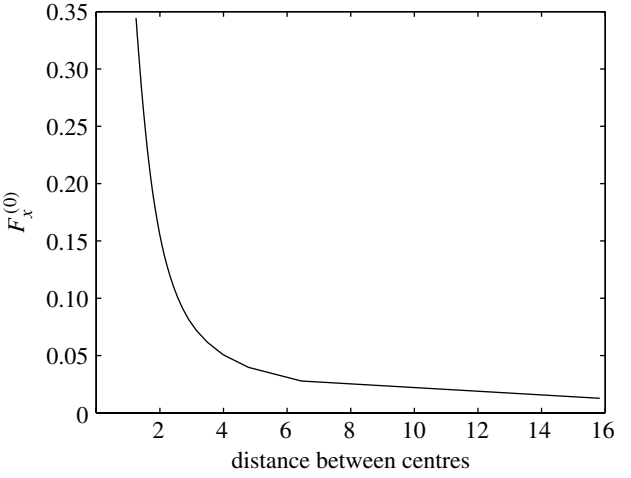

Figure 6. Graph of horizontal force on the right-most aerofoil in the horizontally aligned configuration with $U=1$, $\chi=0$, $\Gamma_0=\Gamma_1=-1$. The two aerofoils repel each other horizontally with a force that increases as the separation of the aerofoils decreases. The vertical force on each cylinder is found to equal -1 for all values of their separation.

9. The case of three (triplane) aerofoils

This section studies the effect of adding a third aerofoil (even more aerofoils can be added, if desired, and be treated analogously). Such considerations are relevant to the study of lift on triplane aerofoils (Munk 1927).

Consider the case of streaming flow around three circular aerofoils. The conformal map to be used in the following examples is

$$z(\zeta) = \frac{\alpha}{\zeta - \beta} + \gamma, \tag{9.1}$$

where β is chosen arbitrarily while the real parameters α and γ are chosen to ensure that the image of C_0 is a unit radius cylinder centred at the origin in the z-plane. In all the following calculations we take $U=1$ and $\rho=1$.

(a) *Unstaggered triplane aerofoils*

Figure 7 shows the steady streamline distribution for uniform potential flow, in the direction of the x-axis, past three equal-sized cylindrical aerofoils aligned vertically. There are two pre-image circles C_1 and C_2 inside the unit disc in this case and C_0 is taken to map to the central aerofoil. C_1 is taken to map to the lower aerofoil. In the first diagram the round-aerofoil circulations are all zero with subsequent diagrams showing various instances in which the round-aerofoil circulations are no longer zero. In the second diagram, the circulations are all equal and taken to be -5. In this case, there are two stagnation points on the lower side of each aerofoil. In the next diagram, the circulations are again equal but are taken to be -15. These circulations are sufficiently strong that, while there are still two stagnation points on the upper two aerofoils, the two stagnation points that were on the lower aerofoil have now moved off the aerofoil and into the flow to produce a single stagnation point below the aerofoil

configuration. In the fourth diagram of figure 7, the round-aerofoil circulations have all been increased to -25. Now, the two stagnation points on the middle aerofoil have also moved off into the flow.

As for the forces exerted on the aerofoils, for all cases shown in figure 7 it is found that the net horizontal force on each aerofoil is zero. There is therefore no drag on any of the aerofoils. Again, this follows from the fore–aft symmetry of the flow. Figure 8 shows the vertical lift forces $F_y^{(j)}, j=0,1,2$, on the aerofoils as a function of the separation of their centres in the case where all the round-aerofoil circulations are equal to -1. As the separation gets large, so that the interaction effect between aerofoils is slight, the lift tends to the Kutta–Joukowski value of $-\rho\Gamma U=1$, as expected. As the separation distance decreases it is found that the lift forces diverge from this value with the lifts on the upper cylinder always being greatest. The sum of the vertical forces on all three aerofoils is again found to always equal three irrespective of the separations of the aerofoils. It is interesting to note that, when the separation is sufficiently small, the vertical force on the lowest aerofoil actually becomes negative thus corresponding to a down-thrust instead of a lift. This is because, even without circulation, there is a net down-thrust on the upper aerofoil which gets larger as the aerofoils get closer together. For sufficiently small separations, the circulation imposed in this case is not large enough to counteract this downward force.

Figure 9 shows the vertical forces on the aerofoils, as a function of the separation of the centres, in the case where all the round-aerofoil circulations are now equal to -5. Again, as the separation gets large, all vertical forces tend to the Kutta–Joukowski value of five although it should be observed that this asymptotic value is reached much more slowly than in figure 8. In this case, however, as the separation decreases the force on the lower aerofoil no longer becomes negative. Indeed, the graphs of the vertical forces on both the upper and lower aerofoils exhibit turning point behaviours. As expected, it is again found that the sum of the vertical forces is 15 irrespective of the separation of the aerofoils.

(*b*) *Tandem triplane aerofoils*

By contrast, figure 10 shows the case of streaming flow past a horizontally aligned arrangement of circular aerofoils (the tandem configuration). The upper diagram of figure 10 shows the case in which all round-aerofoil circulations are zero, the middle and lower diagrams show the cases when the circulations are all equal to -5 and -10, respectively. In the middle diagram each aerofoil exhibits two stagnation points on its surface. In the lower diagram, the two stagnation points on the middle aerofoil have moved off to form a single stagnation point in the flow. There remain, however, two stagnation points on each of the side aerofoils.

As for the forces, the key observation is that now the streamline distribution is no longer symmetric fore and aft of the two side aerofoils in the configuration (although it remains symmetric fore and aft of the central aerofoil). In the zero-circulation case, as expected, there is no lift on any of the aerofoils and no net force at all on the central aerofoil. However, the two side aerofoils experience non-zero net horizontal forces; in fact the aerofoils repel each other. Figures 11 and 12 show the forces on the aerofoils, as a function of aerofoil separation, for

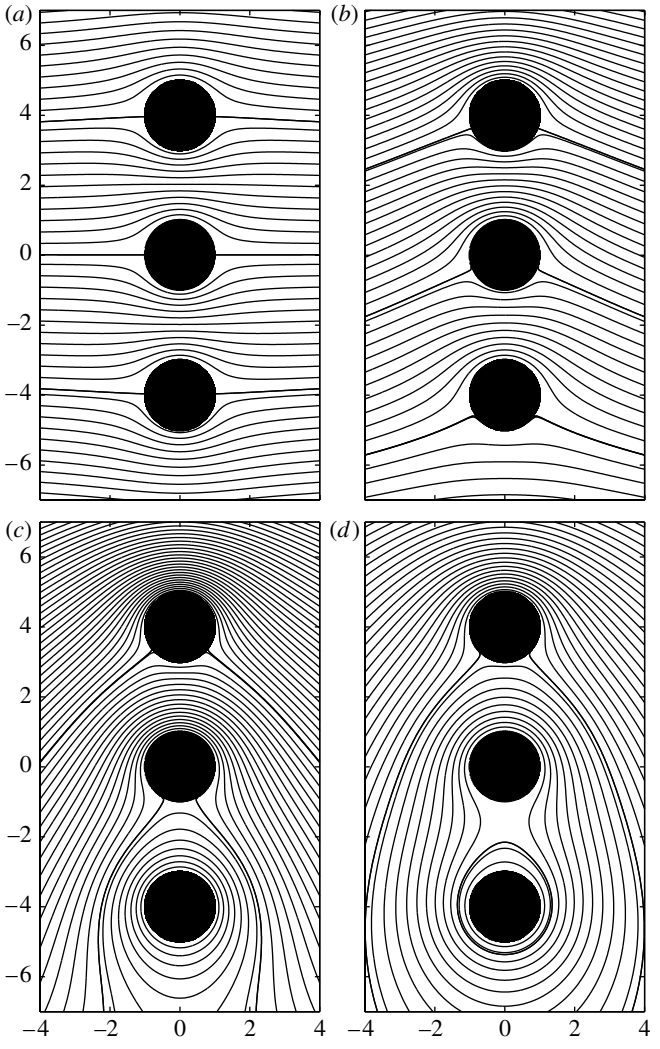

Figure 7. The effect of gradually increasing the round-aerofoil circulations. Here, $U=1$ with (*a*) $\Gamma_0=\Gamma_1=\Gamma_2=0$, (*b*) $\Gamma_0=\Gamma_1=\Gamma_2=-5$, (*c*) $\Gamma_0=\Gamma_1=\Gamma_2=-15$, (*d*) $\Gamma_0=\Gamma_1=\Gamma_2=-25$. Streamlines drawn at intervals of 0.3.

round-aerofoil circulations equal to -1 and -5. As the circulation becomes increasingly negative, the lift on the aerofoils becomes non-zero and equal in magnitude in the case of the two side aerofoils. The latter lift forces are always slightly greater than that on the central aerofoil. Again, the lift forces tend to the respective Kutta–Joukowski values as the separation between the aerofoils gets large. As the separation decreases, the horizontal forces on the two side aerofoils is found to increase in magnitude.

There is no difficulty in adding more aerofoils. One simply considers circular pre-image domains D_ζ with greater numbers of excised circular regions thereby increasing the connectivity of the pre-image domain. It is worth emphasizing that, although no illustrative examples have been given, the formulae can also be

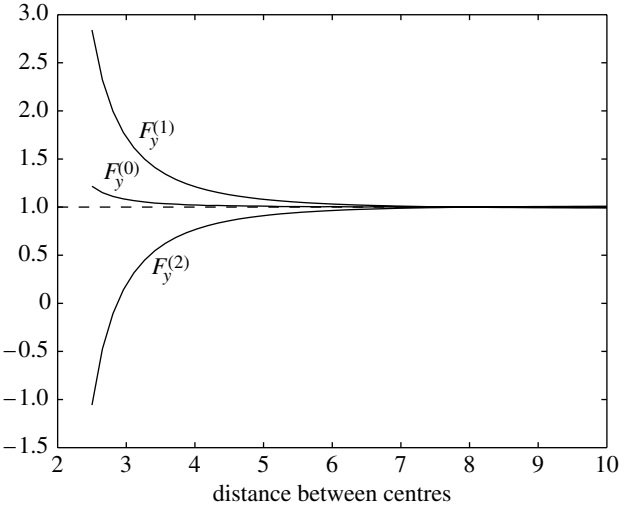

Figure 8. Forces on a vertical array of three cylinders with $U=1$, $\Gamma_0=\Gamma_1=\Gamma_2=-1$ given as a function of the separation distance between centres.

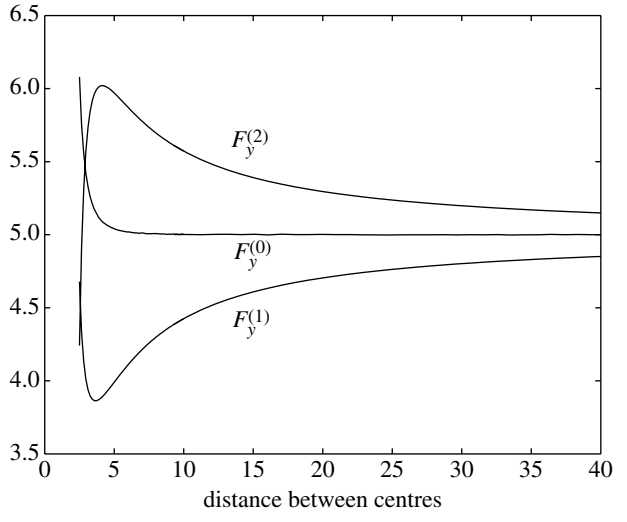

Figure 9. Forces on a vertical array of three cylinders with $U=1$, $\Gamma_0=\Gamma_1=\Gamma_2=-5$ given as a function of the separation distance between centres.

used to analyse more general aerofoil configurations (this is, ones that are not necessarily aligned horizontally or vertically) as well as streaming flows with non-zero angles of attack (that is, $\chi\neq 0$).

10. Discussion

This paper has presented the mathematical generalization, to an arbitrary number of circular aerofoils, of the classic solution of Lagally (1929) for the steady streaming flow past two circular aerofoils with circulation. An analytical

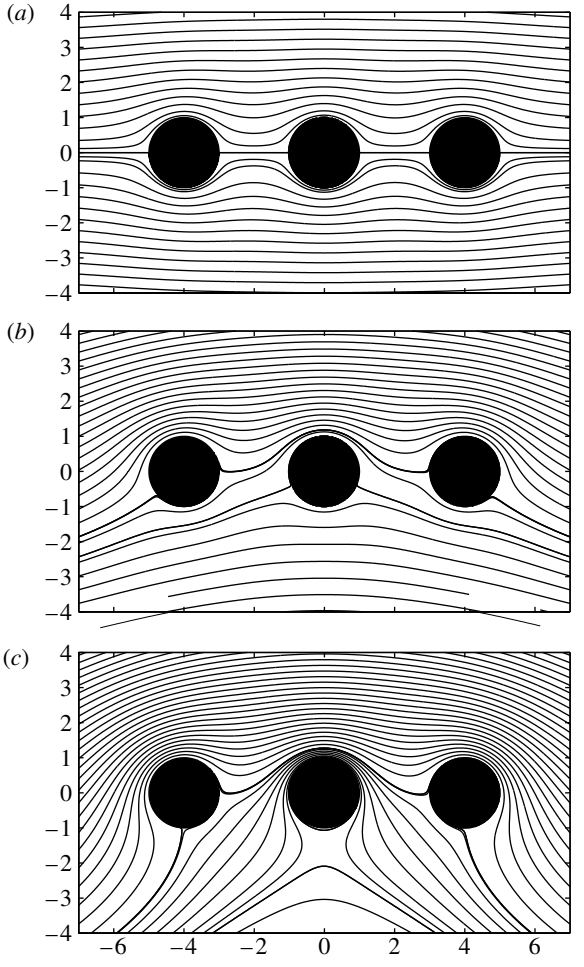

Figure 10. Uniform flow past three equal cylinders with centres separated by four. $U=1$ with $\Gamma_0=\Gamma_1=\Gamma_2=0$ (a), -5 (b) and -10 (c) with $\chi=0$. Streamlines drawn at intervals of 0.3.

approach to finding the complex potentials of the flow around a finite array of aerofoils in a parametric ζ-plane has been devised. This leads to analytical expressions for the integrand in the Blasius integral which can then be readily integrated numerically to determine the forces on the circular aerofoils.

The case of multiple circular aerofoils has been analysed in detail for two reasons. The first is that the mathematical solutions to such problems have not, to the best of our knowledge, been previously recorded in the literature (beyond Lagally's two circle solution (Lagally 1929)). The second is that the conformal mappings $z(\zeta)$ from D_ζ to the fluid region D_z assume a particular simple form in this case. Physically, of course, aerofoils of more realistic ('streamlined') shape are of interest and it should be clear that, in principle, aerofoils with more complicated geometries can be treated by the same methods. To treat such cases analytically, however, the functional form of the relevant conformal mapping $z(\zeta)$ must be found. The challenges encompassed in the determination of the relevant conformal mappings $z(\zeta)$ to monoplane and biplane aerofoils should not

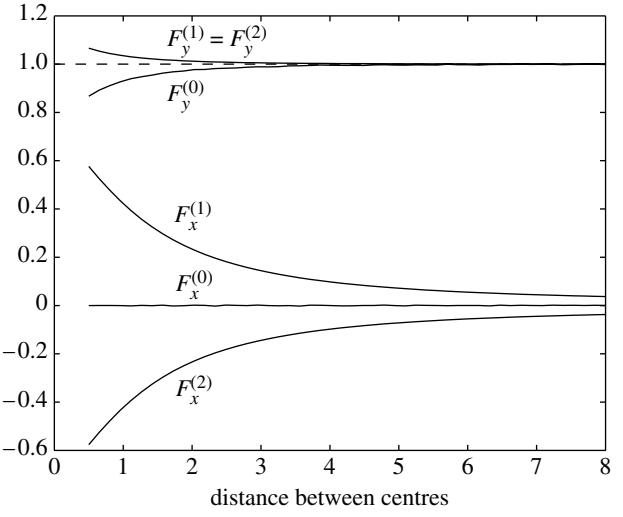

Figure 11. Forces on a horizontal array of three cylinders with $U=1$, $\Gamma_0=\Gamma_1=\Gamma_2=-1$ given as a function of the separation distance between centres.

be underestimated. Indeed, this very problem has commanded a large amount of attention in the wing theory literature. Theodorssen (1932) and Garrick (1936) made seminal contributions in this area. Theodorssen (1932) devised numerical methods based on mapping a monoplane aerofoil to a near-circle and then iterating towards a conformal mapping that takes this near-circle to an exact circle. Garrick (1936) extended this to the biplane case and, unsurprisingly, to complete the solution, combined his conformal mapping construction with Lagally's solution. Further contributions in this area have been made by Theodorssen & Garrick (1933) and Ives (1976).

While we have focussed on streaming flows past aerofoils, analogous flow problems arise in geophysical applications where the motion of vortices around topography is of great interest. Such problems are relevant, for example, in the modelling the motion of oceanic eddies around topography (such as islands, headlands and coastlines). Indeed, this provided the motivation for the study by Johnson & McDonald (2004) on the motion of point vortices (and vortex patches) around two circular islands. In their study, the motion of the vortex in the presence of imposed background flows and non-zero round-island circulations was also computed. Recently, Crowdy & Marshall (2005*a*,*b*) have presented a generalized theory of point vortex motion in fluid domains having any finite connectivity in the special case in which there are no imposed background flows and in which all the round-island circulations vanish. This is the simplest manifestation of a general theory expounded originally, in multiply connected domains, by Lin (1941). Significantly, if one wishes to incorporate the effects of non-zero background flows and non-zero round-island circulations, it turns out that additional contributions arising from these sources (referred to by Lin as due to 'external agencies' (Lin 1941)) can simply be added to the Hamiltonians already found in Crowdy & Marshall (2005*a*). These additions to the Hamiltonian are given in terms of the complex potentials for the background flows and round-island circulations. But such

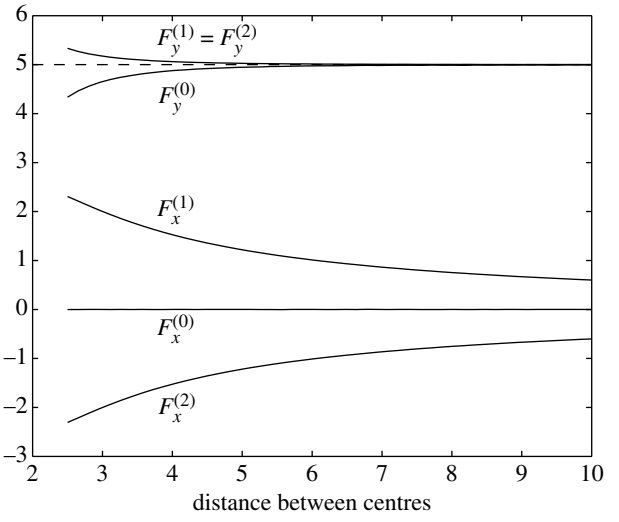

Figure 12. Forces on a horizontal array of three cylinders with $U=1$, $\Gamma_0=\Gamma_1=\Gamma_2=-5$ given as a function of the separation distance between centres.

complex potentials are exactly what have been derived, in analytical form, in the present paper. Thus, the results here can be combined with the analysis in Crowdy & Marshall (2005*a*,*b*) to give a very general analytical framework in which to study the motion of point vortices (any number thereof) in multiply connected domains (of arbitrary finite connectivity) and including the effects of background flows and non-zero circulations around the obstacles/islands.

Finally, it should be mentioned that there has been much recent interest (Burton *et al.* 2004; Wang 2004) in computing the interaction of two *moving* cylindrical obstacles interacting in a potential flow. It is therefore of some interest to extend the methodology of the present paper to incorporate the effect of unsteady relative motion when more than two cylindrical obstacles are present.

The author acknowledges useful discussions with J. S. Marshall.

References

Acheson, D. 1990 *Elementary fluid dynamics*. Oxford: Oxford University Press.

Baker, H. 1995 *Abelian functions*. Cambridge, UK: Cambridge University Press.

Burton, D. A., Gratus, J. & Tucker, R. W. 2004 Hydrodynamic forces on moving discs. *Theor. Appl. Mech.* **31**, 153–188.

Crowdy, D. G. In press. Analytical solutions for uniform potential flow past multiple cylinders. *Eur. J. Mech. B. Fluids*.

Crowdy, D. G. & Marshall, J. S. 2005*a* Analytical formulae for the Kirchhoff-Routh path function in multiply connected domains. *Proc. R. Soc. A* **461**, 2477–2501. (doi:10.1098/rspa.2005.1492)

Crowdy, D. G. & Marshall, J. S. 2005*b* The motion of a point vortex around multiple circular islands. *Phys. Fluids* **17**, 056602. (doi:10.1063/1.1900583)

Ferrari, C. 1930 Sulla trasformazione conforme di due cerchi in due profile alari. *Memorie della Reale Accad. della Scienze di Torino, Serie II* **67**.

Garrick, I. E. 1936 Potential flow about arbitrary biplane wing sections. *NACA Techn. Rep.* **542**.

Glauert, H. 1947 The elements of aerofoil and airscrew theory. *Cambridge Science Classics Series*, 2nd edn. Cambridge, UK: Cambridge University Press.

Ives, D. C. 1976 A modern look at conformal mapping including multiply connected regions. *AAIA J.* **14**, 1006–1011.

Johnson, E. R. & Robb McDonald, N. 2004 The motion of a vortex near two circular cylinders. *Proc. R. Soc. A* **460**, 939–954. (doi:10.1098/rspa.2003.1193)

Lagally, M. 1929 Die reibungslose strömung im aussengebiet zweier kreise. *Z. Angew. Math. Mech.* **9**, 299–305. (English translation in NACA Technical Memorandum, 626, 1932.)

Lin, C. C. 1941 On the motion of vortices in two dimensions. I. Existence of the Kirchhoff-Routh function. *Proc. Natl Acad. Sci.* **27**, 570–575.

Milne-Thomson, L. 1968 *Theoretical hydrodynamics*. New York: Macmillan.

Munk, M. M. 1927 The air forces on a systematic series of biplane and triplane cellule models. *NACA Techn. Rep.* **256**.

Nehari, Z. 1952 *Conformal mapping*. New York: McGraw-Hill.

Robinson, A. 1956 *Wing theory*. Cambridge, UK: Cambridge University Press.

Theodorssen, T. 1932 Theory of wing sections of arbitrary shape. *NACA Tech. Rep.* **411**.

Theodorssen, T. & Garrick, I. E. 1933 General potential theory of arbitrary wing sections. *NACA Techn. Rep.* **452**.

Wang, Q. X. 2004 Interaction of two circular cylinders in inviscid fluid. *Phys. Fluids* **16**, 4412–4425. (doi:10.1063/1.1804536)

Whittaker, E. T. & Watson, G. N. 1927 *A course of modern analysis*. Cambridge, UK: Cambridge University Press.

Yamamoto, T. 1976 Hydrodynamic forces on multiple circular cylinders. *J. Hydraulics Div. Proc. Am. Soc. Civil Eng.* **102**, 1193–1211.